scientific reports

Check for updates

OPEN

Isoniazid preventive therapy modulates *Mycobacterium tuberculosis*-specific T-cell responses in individuals with latent tuberculosis and type 2 diabetes

Phillip Ssekamatte[1,2]✉, Diana Sitenda[1], Rose Nabatanzi[1], Marjorie Nakibuule[2], Davis Kibirige[3], Andrew Peter Kyazze[4], David Patrick Kateete[1], Bernard Ssentalo Bagaya[1], Obondo James Sande[1], Reinout van Crevel[5], Stephen Cose[2] & Irene Andia Biraro[2,4]

Diabetes mellitus (DM) is a significant contributor to tuberculosis (TB) incidence and poor treatment outcomes. This study explored the impact of isoniazid preventive therapy (IPT) on *Mycobacterium tuberculosis* (*Mtb*)-specific T-cell memory phenotypes and function among participants with latent TB infection and DM (LTBI-DM) at baseline and after 6 months of IPT; and compared the responses to healthy controls (HC). Peripheral blood mononuclear cells were stimulated with ESAT-6 and CFP-10 peptide pools to analyse $CD4^+$ and $CD8^+$ T-cell responses using flow cytometry. In LTBI-DM participants, effector memory $CD4^+$ and $CD8^+$ T cells were decreased post-IPT, suggesting a shift towards a less-activated state or differentiation into other subsets. CXCR5 expression on both $CD4^+$ and $CD8^+$ T cells was upregulated, while PD-1 expression was downregulated post-IPT, indicating reduced T-cell exhaustion and improved homing capabilities. Lastly, IL-17 A and IL-13 production in $CD4^+$ and $CD8^+$ T cells was increased post-IPT, respectively, which play a role in enhanced *Mtb* infection control. The post-IPT T-cell alterations were similar to normal HC levels. These findings suggest that IPT modulates and normalises specific T-cell memory phenotypes and functional responses in LTBI-DM participants, potentially contributing to improved long-term immunity and protection against TB. This study highlights the importance of preventive therapy in high-risk populations, and larger studies with more extended follow-up are needed to assess long-lasting IPT effects.

Keywords Latent TB infection, Diabetes, T cells, Isoniazid preventive treatment, Memory phenotypes, Functional profiles

In recent years, diabetes mellitus (DM) has been recognised as a significant contributor to tuberculosis (TB) incidence and poor treatment outcomes[1]. Diabetes mellitus increases the risk of progression from latent TB infection (LTBI) to active TB (ATB) by 3-fold[1]. Tuberculosis is a preventable infectious disease caused by the bacilli *Mycobacterium tuberculosis* (*Mtb*) and predominantly affects the lung primary alveolus[2]. Despite significant efforts towards its control, TB remains a persistent global health concern[2]. Globally, in 2023, the World Health Organisation (WHO) reported that approximately 10.8 million incident TB cases, of which about 1.25 million people died[2]. This increased susceptibility is attributed to impaired immune responses, including deficits in myeloid function, T and B-cell responses, and cytokine production[3–6].

The interaction between *Mtb* and host immune responses, particularly with lymphocytes, is central to understanding the pathophysiology of *Mtb* in DM participants[4,6]. T-cell-mediated immunity is pivotal in controlling *Mtb* infection by recognising *Mtb* antigens and orchestrating immune responses that limit bacterial

[1]Department of Immunology and Molecular Biology, School of Biomedical Sciences, College of Health Sciences, Makerere University, Kampala, Uganda. [2]Medical Research Council/Uganda Virus Research Institute and London School of Hygiene & Tropical Medicine Uganda Research Unit, Entebbe, Uganda. [3]Department of Medicine, Uganda Martyrs Hospital Lubaga, Kampala, Uganda. [4]Department of Internal Medicine, School of Medicine, College of Health Sciences, Makerere University, Kampala, Uganda. [5]Department of Internal Medicine and Radboud Centre for Infectious Diseases, Radboud University Medical Centre, Kampala, Uganda. ✉email: psekamate@gmail.com

growth[7–10]. However, DM-induced hyperglycaemia can impair the functional profiles of T cells, leading to insufficient production of effector cytokines[11]. Diabetes mellitus has been reported to impair $CD8^+$ T-cell multifunctionality by promoting increased PD-1 expression that hampers cellular cytotoxicity and cytokine production[12], specifically decreasing the proportion of IFN-γ+IL-2+TNF cells[12]. Treatment with metformin has been shown to reverse these DM-induced effects[12]. We have previously shown that DM promotes T-cell exhaustion and decreases both the activation profile of $CD4^+$ T cells and polyfunctionality of *Mtb*-specific $CD4^+$ as well as their central and effector memory T-cell responses[13]. This immunological perturbation during DM might contribute to the increased risk of LTBI re-activation and promote the potential for more severe disease progression[5,14]. The increased susceptibility of participants with DM to LTBI highlights the significance of implementing effective preventive measures.

Tuberculosis preventive treatment (TPT), including isoniazid (INH) preventive therapy (IPT), is a cornerstone of TB control strategies and is known to reduce the risk of TB[15]. TPT modulates the *Mtb*-specific immune responses in participants with active TB and Human Immunodeficiency Virus (HIV)[16]. Antigen-specific $CD4^+$ T cells become less differentiated, with decreased PD-1 and CTLA4 expression and subtle changes in cytokine and chemokine functional responses following TB treatment[16]. Anti-TB treatment has been reported to decrease antigen-specific T-cell naïve and effector memory responses at month 2 but not month 6 among participants with ATB-DM[17]. However, the impact of TPT, particularly IPT, on *Mtb*-specific T-cell memory phenotypes and functional responses in LTBI-DM participants remains poorly characterised. We hypothesised that IPT in LTBI-DM participants modulates impaired *Mtb*-specific T-cell memory phenotypes and functional responses towards improved protection against *Mtb*.

Materials and methods

Ethics statement

Informed consent was obtained from all subjects and/or their legal guardian(s) before they were enrolled in the Tuberculosis and Diabetes (TAD) and Kampala TB (KTB) studies. TAD and KTB studies were approved by the institutional review boards, including the School of Biomedical Sciences Research and Ethics Committee (SBS-REC), Makerere University (TAD reference number: SBS-398), the School of Medicine Research and Ethics Committee (SOM-REC), Makerere University (KTB reference number: 2011 – 125) and the Uganda National Council for Science and Technology (UNCST) (TAD, reference number: HS66ES and KTB, reference number: HS676). Ethical approval for this study was obtained from SBS-REC, reference number SBS-2021-41 and UNCST, reference number HS1696ES. All data were anonymised. All methods were performed in accordance with the relevant guidelines and regulations.

Participants

Participants with LTBI and DM (LTBI-DM) were enrolled in an exploratory nested cohort between January and December 2019 from Kiruddu National Referral Hospital in Kampala, Uganda. This cohort was part of the TAD study[3], a longitudinal study that monitored Isoniazid treatment adherence of participants with LTBI-DM and those with active TB. Healthy control [(HC); no LTBI & no DM] participants were enrolled in a TB household contact cohort KTB study at Kisenyi and Kitebi Health Center IVs from May 2011 to January 2012, as previously described[18]. The KTB study did not collect DM-related participant characteristics. The HC participants were included to provide baseline T-cell responses. All participants underwent a TB symptom screen to rule out active TB. Following the manufacturer's recommendations, LTBI was diagnosed using a positive QuantiFERON-TB Gold (QFT)-Plus assay for TAD study. For KTB study, LTBI was ruled out using the QFT In-Tube assay. Diabetes mellitus was diagnosed based on glycated haemoglobin (HbA1c) levels ≥ 6.5%. All the participants were HIV seronegative and anti-tuberculous treatment naïve. A total of 28 LTBI-DM participants received IPT for 6 months. Blood samples were collected at baseline (M0; before IPT) and 6 months (M6; after IPT) for LTBI-DM participants. A total of 17 HC participants were included as controls.

PBMC isolation

Briefly, 10 ml of heparinised blood collected by venepuncture was transported within 4 h to the immunology laboratories at the College of Health Sciences Makerere University and the MRC/UVRI and LSHTM Uganda Research Unit. The PBMCs and plasma were isolated using Ficoll-Histopaque density gradient centrifugation. The Cells were counted and resuspended in cold foetal bovine serum (FBS) supplemented with 10% dimethyl sulfoxide (DMSO). Cells were then adjusted to a final concentration of 3×10^6 cells/ml and transferred to a cold Mr Frosty™ freezing container overnight at -80°C. They were later transferred to liquid nitrogen (-197°C), while the plasma was stored at -80°C for long-term storage.

Cell stimulation and culture

Upon retrieval from liquid nitrogen, participant frozen cell vials (3×10^6) at baseline and 6 months after IPT were thawed in a 37°C water bath and later transferred to R20 (Roswell Park Memorial Institute [RPMI] with 20% FBS, 1% Penicillin/streptomycin, 2mM L-Glutamine, 15mM HEPES buffer) media. The PBMCs were then rinsed and rested in R20 media in a humidified incubator at 5%CO_2, 37°C for 4 h. The cells (200 µl/2×10^6, resuspended in R20) were stimulated in a humidified incubator at 37°C, 5%CO_2 for 18 h (overnight) with *Mtb*-specific peptide pools of early secreted antigenic target-6 kDa [ESAT-6 (21-peptide array; 10 µg/ml)], and culture filtrate protein-10 kDa [CFP-10 (22-peptide array; 10 µg/ml)], all from BEI Resources (Manassas, VA). The peptides consist of 15- or 16-mers peptides (overlapping by 11 or 12 amino acids) spanning the entire amino acid sequences for the ESAT-6 and CFP-10. Phytohemagglutinin-lectin (PHA-L [10 µg/ml, Millipore, Sigma]) was used as a positive control, and unstimulated cells (R20 media) as a negative control. Stimulations were performed for 3 h, after which Brefeldin A (5 µg/ml, BioLegend) was added to all tubes. Cells were further

incubated and stimulated for 15 h. All experiments were performed in the presence of co-stimulatory antibodies, anti-CD28 and anti-CD49d (1 µg/ml each, BD Biosciences) and CD107a PE-Cy5 (H4A3, BD Biosciences) antibody for the 18 h.

Cell staining

After stimulations, cells were washed with Dulbecco's phosphate-buffered saline (PBS [1X, Sigma-Aldrich]), followed by staining with a fixable viability dye, Zombie Aqua (BioLegend) at room temperature for 20 min in the dark. Cells were washed and resuspended in cell staining buffer (BioLegend), then blocked for Fc receptors using BD Fc block (2.5 µg/ml, BD Biosciences) at room temperature for 10 min in the dark. Cells were surface stained at 4 °C for 30 min in the dark with the following antibodies: CD3 FITC (OKT3), CD4 APC-Cy7 (OKT4), CD8 BV650 (SK1), CCR7 PE-Dazzle 594 (G043H7), CD45RA BV421 (HI100), HLA-DR BV605 (L243), all from BioLegend, and PD-1 PE-Cy7 (EH12.1), and CXCR5 APC-R700 (RF8B2) from BD Biosciences. For intracellular cytokine staining, cells were washed, fixed using fixation buffer (4% paraformaldehyde, BioLegend), and permeabilised using working strength intracellular staining permeabilisation wash buffer (1X, BioLegend) according to manufacturer's recommendations. Fixed cells were intracellularly stained at room temperature for 20 min in the dark with the following antibodies: IFN-γ APC (B27), IL-13 PE (JES10-5A2), all from BD Biosciences, and IL-17 A BV785 (BL168) from BioLegend. The cells were immediately acquired on the Cytek Aurora spectral flow cytometer (Cytek Biosciences). The flow cytometry antibody panel, including the clone and catalogue number, is shown in Table 1.

ELISA

The human CXCL13/BLC/BCA-1 Quantikine ELISA Kit (R&D Systems, Inc. Minneapolis, MN) was used to measure the amount of natural and recombinant human CXCL13 in the plasma of LTBI-DM participants before and after IPT. Standards, controls, and samples were run in duplicate. Results were measured at 450 and 570 nm using the Synergy LX multimode reader system (BioTek, Agilent). After background subtraction, concentrations were determined using the standard curve generated using Gen5 software (version 2.71.2, BioTek, Agilent) based on the manufacturer's recommendations.

Data and statistical analysis

All flow cytometry data were analysed using FlowJo (version 10.10.0; BD Biosciences, San Jose, CA, USA) for Mac. Gating was standardised and set using Fluorescence Minus One (FMO) and compensation controls to correct for spectral overlap. The gating strategy is shown in Fig. 1. Data analysis and statistical tests were performed using R (version 4.4.3; R Foundation for Statistical Computing, Vienna, Austria). Using the ComBat function from the surrogate variable analysis (sva; version 3.54.0) package, no batch effects were detected between LTBI-DM and HC participant samples. The package ggplot2 (version 3.5.1) was used for data visualisation. To compare the *Mtb*-specific $CD4^+$ and $CD8^+$ T-cell memory phenotypes and functional profiles, as well as the CXCL13 expression between LTBI-DM participants at M0 and M6, we used the Wilcoxon matched-pairs signed rank test, else Mann-Whitney U test was performed between HC and M0/M6 for LTBI-DM and HC participants. Data were represented by a dot plot to show single-sample behaviour, a violin plot to define group distribution behaviour, and a box plot to display the confidence interval around the median, with a box boundary defining the IQR and whiskers showing 1.5×IQR. The grey lines depict individual participant phenotype trajectories from M0 to M6, while the red line represents the aggregate median trend across all participants over the same period. A p-value < 0.05 was considered statistically significant.

After cell surface and intracellular cytokine staining, single cells were acquired on the Cytek Aurora flow cytometer. All flow cytometry data were analysed using FlowJo (v10.10.0) for Mac. Gating was standardised and set using Fluorescence Minus One (FMO) controls and compensation controls to correct for spectral overlap. To identify *Mtb*-specific $CD4^+$ and $CD8^+$ T cells phenotype and functional responses, we first gated on single cells, followed by lymphocytes, then $CD3^+$ gate in combination with live cells. T-cell populations were identified with

Role	Marker	Fluorochrome	Clone	Catalogue No.	Manufacturer
Cell viability	Live Dead	Zombie aqua	N/A	423,101	BioLegend
Lineage	CD3	FITC	OKT3	317,306	BioLegend
	CD4	APC-Cy7	OKT4	317,418	BioLegend
	CD8	BV650	SK1	344,730	BioLegend
Memory	CD45RA	BV421	HI100	304,130	BioLegend
	CCR7	PE-Dazzle 594	G043H7	353,236	BioLegend
Activation	HLA-DR	BV605	L243	307,640	BioLegend
Exhaustion	PD-1	PE-Cy7	EH12.1	561,272	BD Biosciences
Degranulation	CD107a	PE-Cy5	H4A3	555,802	BD Biosciences
Homing	CXCR5	APC-R700	RF8B2	565,191	BD Biosciences
Intracellular cytokines	IFN-γ	APC	B27	554,702	BD Biosciences
	IL-13	PE	JES10-5A2	559,328	BD Biosciences
	IL-17 A	BV785	BL168	512,338	BioLegend

Table 1. Flow cytometry panel.

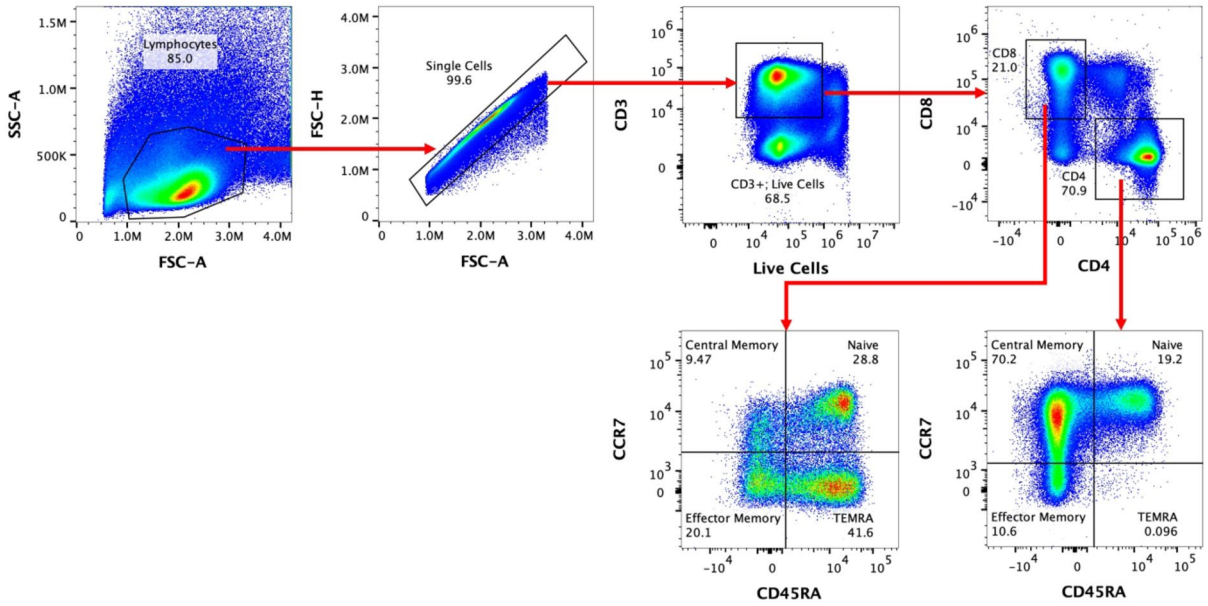

Fig. 1. Gating strategy to identify *Mtb*-specific CD4$^+$ and CD8$^+$ T cells in participant PBMC samples.

traditional gates on CD4 and CD8. T-cell memory responses were then identified based on CD45RA and CCR7 gates. Functional markers (IFN-γ, IL-13, IL-17 A, CD107a, HLA-DR, PD-1) were then gated independently on CD3$^+$CD4$^+$ and CD3$^+$CD8$^+$ T cells.

Results

Description of participant characteristics

A total of 28 LTBI-DM (71.4% female) and 17 HC (58.8% female) participants were included, as shown in Table 2. The LTBI-DM participants were older (median age 48.0 [25.0–69.0] years) compared to HC participants (31.0 [26.0–42.0] years). Among the LTBI-DM group, the median number of children was 5.0 (2.0–17.0), and a higher proportion reported alcohol use (21.4% vs. none among HC). The median BMI was also higher in the LTBI-DM (27.7 [16.9–40.2] kg/m^2 vs. 25.3 [22.3–31.7] kg/m^2), consistent with elevated waist and hip circumferences measured only in LTBI-DM participants. Reflecting their diabetic status, the LTBI-DM participants showed elevated fasting blood glucose (11.1 [4.0-31.2] mmol/L) and HbA1c (9.2% [4.0–15.0]) levels, and all received medications (primarily metformin alone or with glibenclamide). By month 6, the LTBI-DM median HbA1c had decreased to 7.9% (6.5–9.9), reflecting ongoing clinical management of DM. Most LTBI-DM participants (78.6%) and controls (94.1%) had a BCG scar, and while 89.3% of LTBI-DM participants had no prior TB history, all HC participants also reported no TB history.

IPT decreases *Mtb*-specific CD4$^+$ and CD8$^+$ T-cell effector memory phenotypes in LTBI-DM participants

We performed a phenotypic analysis of CD4$^+$ and CD8$^+$ T-cell subsets of participant PBMC samples with LTBI-DM and HC. Flow cytometry was used to classify *Mtb*-specific T-cell memory phenotypes into four categories based on the expression of CD45RA and CCR7 as a percentage of total CD4$^+$ and CD8$^+$ T cells. The T-cell memory phenotypes were defined as: central memory (CM; CD45RA$^-$CCR7$^+$), naïve (CD45RA$^+$CCR7$^+$), terminally differentiated effector memory (TEMRA; CD45RA$^+$CCR7$^-$), and effector memory (EM; CD45RA$^-$CCR7$^-$) (Fig. 1). For LTBI-DM participants, effector memory CD4$^+$ T cells were significantly decreased from M0 to M6 [median (IQR); 11.55 (7.78–15.45): 11.30 (6.60-23.78); $p = 0.043$] (Fig. 2C). Similarly, effector memory CD8$^+$ T cells were significantly decreased from M0 to M6 [30.85 (16.33–45.25): 20.15 (13.95–34.43); $p = 0.031$] (Fig. 2G). In comparison, the EM CD4$^+$ and CD8$^+$ T-cell frequencies in HC participants were 12.20 (8.30–14.2) and 25.00 (18.70–28.70), respectively, and non-significant from M0 and M6 (Fig. 2C and G). No significant trends were observed for the CD4$^+$ and CD8$^+$ Naïve, Central Memory and TEMRA T cells in the LTBI-DM and HC participants (Fig. 2A, B, D, E, F, H).

PBMCs were stimulated and cultured for 18 h with ESAT-6 and CFP-10 peptide pools plus brefeldin A and stained for surface markers. (B-E and G-J) Representative combined dot-violin-box plots depicting the percentage expression of naïve, central memory, effector memory and TEMRA phenotypes in CD4$^+$ and CD8$^+$ T cells before and post-IPT in LTBI-DM; and HC participants. The grey lines depict individual participant phenotype trajectories from M0 to M6, while the red line represents the aggregate median trend for LTBI-DM participants over the same period. Size of group: LTBI-DM ($n = 24$), HC ($n = 17$). Wilcoxon matched-pairs signed rank and Mann-Whitney U tests were performed to determine the statistical significance between M0 and M6 for LTBI-DM, as well as between HC and M0/M6, respectively. $^*p < 0.05$. Non-significant (ns) p-values were not shown.

	LTBI-DM; M0 ($n=28$)	HC ($n=17$)
Sex		
Female / Male	20 (71.4%) / 8 (28.6%)	10 (58.8%) / 7(41.2%)
Age*	48.0 (25.0–69.0)	31.0 (26.0–42.0)
Occupation		
Business	14 (50.0%)	10 (58.8%)
Farmer	1 (3.6%)	0
Skilled labourer	1 (3.6%)	0
Teacher	2 (7.1%)	0
Truck driver / Unskilled	2 (7.1%)	2 (11.8%)
Unemployed	5 (17.9%)	5 (29.4%)
Number of children*$	5.0 (2.0–17.0)	
Smoking		
Yes / No	2 (7.1%) / 23 (82.1%)	1 (5.9%) / 16 (94.1%)
Alcohol		
Yes / No	6 (21.4%) / 19 (67.9%)	0 (0.0%) / 17 (100.0%)
History of TB		
No	25 (89.3%)	No (100.0%)
TB contact		
No	21 (75.0%)	0 (0.0%)
Not sure	3 (10.7%)	0 (0.0%)
Yes	1 (3.6%)	17 (100.0%)
Weight (Kg)*	72.2 (41.0-107.5)	68.0 (58.0-73.5)
Height (m)*	1.6 (1.5-2.0)	1.6 (1.5–1.7)
BMI (Kg/m^2)*	27.7 (16.9–40.2)	25.3 (22.3–31.7)
Waist circumference (cm)*$	94.0 (67.0-118.0)	
Hip circumference (cm)*$	100.5 (80.0-142.5)	
WHR*$	0.9 (0.7–1.3)	
Systolic blood pressure (mmHg)*$	139.8 (84.0-210.7)	
Diastolic blood pressure (mmHg)*$	89.0 (56.0-118.0)	
BCG scar		
Yes / No	22 (78.6%) / 3 (10.7%)	16 (94.1%) / 1 (5.9%)
FBS (mmol/L)*$	11.1 (4.0-31.2)	
HbA1c (%)*+$	9.2 (4.0–15.0)	
HDL (mmol/L)*$	1.1 (0.7–1.9)	
LDL (mmol/L)*$	3.4 (0.7–4.9)	
Triglycerides (mmol/L)*$	1.7 (0.6–3.3)	
Microalbumin (mg/L)*$	10.0 (10.0-121.5)	
White blood cells (10^3/μL)*$	5.5 (2.9–10.6)	
Neutrophils (10^3/μL)*$	2.7 (1.0-7.6)	
Lymphocytes (10^3/μL)*$	2.2 (1.0-3.6)	
Haemoglobin (g/dL)*$	14.7 (9.4–19.6)	

Table 2. Baseline characteristics of study participants. *Abbreviations*: BMI–Body mass index; WHR–Waist-hip ratio; HbA1c–glycated haemoglobin; FBS–Fasting blood glucose; HDL–High-density lipoprotein; LDL–Low-density lipoprotein. *Ranges depict medians and IQRs; $Data variables were not collected for the HC participants. +*Footnote*: At M6, the median HbA1c for the LTBI-DM participants was 7.9% (6.5–9.9). All LTBI-DM participants took glucose-lowering medications throughout the study follow-up period, primarily metformin alone or in combination with glibenclamide.

IPT increases *Mtb*-specific CD4$^+$ and CD8$^+$ T-cell CXCR5 expression and decreases CXCL13 protein levels in LTBI-DM participants

Next, we assessed the *Mtb*-specific CXCR5 expression and CXCL13 levels to determine the homing capabilities of CD4$^+$ and CD8$^+$ T-cells (Fig. 3). For LTBI-DM participants, CD4$^+$ and CD8$^+$ CXCR5 expression was significantly upregulated post-IPT [16.60 (12.80-18.55): 18.05 (15.63–21.25); $p=0.038$] (Fig. 3B) and [1.79 (1.35–2.40): 2.60 (2.00-3.45); $p=0.006$] (Fig. 3D) respectively. The HC participants showed the CXCR5 expression of 18.05 (15.93–24.05) for CD4$^+$ T cells and a significantly higher CXCR5 expression on CD8$^+$ T cells [3.05 (2.28–3.59); $p=0.012$] compared to LTBI-DM at baseline (Fig. 3B and D). Conversely, high levels of CXCL13

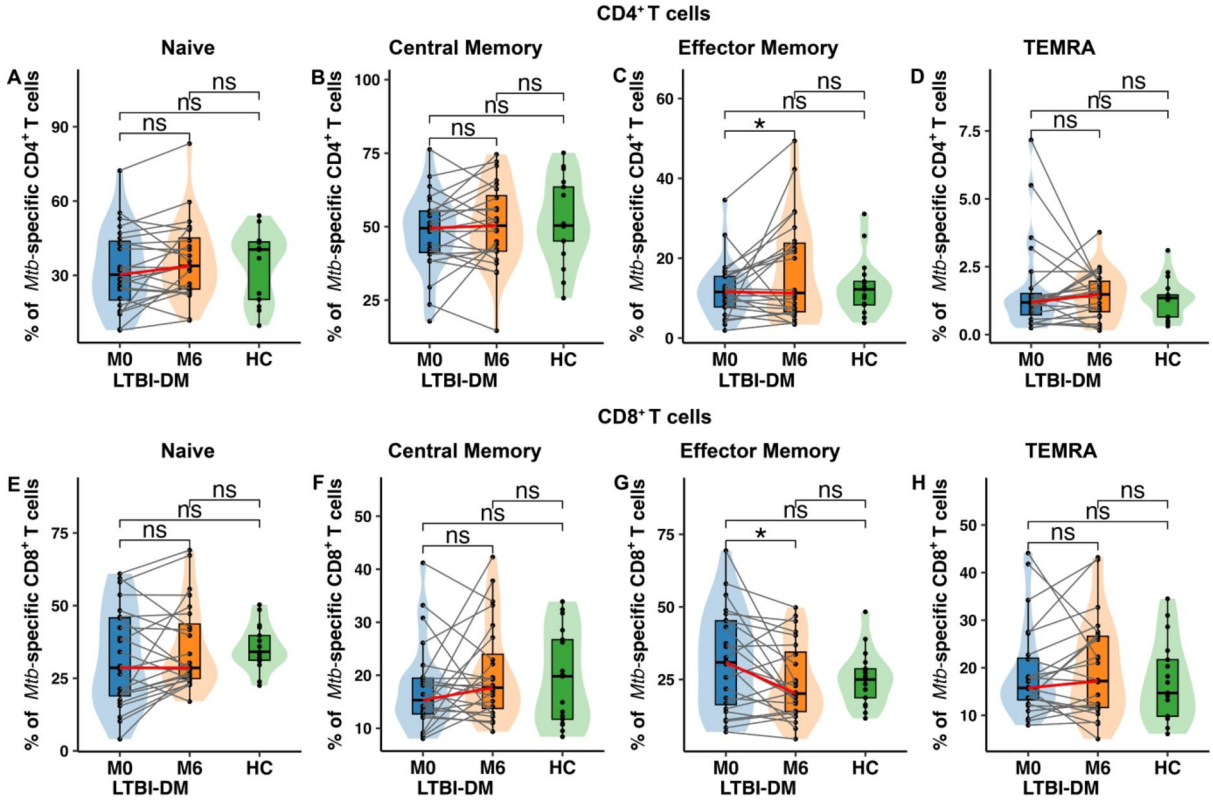

Fig. 2. *Mtb*-specific CD4⁺ and CD8⁺ T-cell memory phenotypes before and after IPT for LTBI-DM; and HC participants.

were measured in the plasma of LTBI-DM participants at baseline, and these decreased significantly post-IPT [35.55 (26.17–44.44): 27.77 (24.07–35.25); $p = 0.007$] (Fig. 3E). Additionally, HC participants had the CXCL13 levels significantly decreased compared to the baseline LTBI-DM participants [21.44 (17.25–35.56) vs. 35.55 (26.17–44.44); $p = 0.013$] (Fig. 3E).

Representative flow cytometry plots are shown for (A and C) CD4⁺ and CD8⁺ CXCR5 expression profiles. PBMCs were stimulated and cultured for 18 h with ESAT-6 and CFP-10 peptide pools plus brefeldin A and stained for surface markers. (B and D) Representative combined dot-violin-box plots depict the percentage expression of functional profiles in CD4⁺ T cells before and post-IPT in LTBI-DM; and HC participants. (E) CXCL13 protein expression levels were measured by ELISA in the plasma of LTBI-DM and DM participants before and post-IPT, as well as the HC. The grey lines depict individual participant phenotype trajectories from M0 to M6, while the red line represents the aggregate median trend for LTBI-DM participants over the same period. Size of group: LTBI-DM ($n = 24$) for CXCR5, LTBI-DM ($n = 28$) for CXCL13, HC ($n = 17$). Wilcoxon matched-pairs signed rank and Mann-Whitney U tests were performed to determine the statistical significance between M0 and M6 for LTBI-DM, as well as between HC and M0/M6, respectively. $p < 0.05$ (*), $p < 0.01$ (**). Non-significant (ns) p-values were not shown.

IPT decreases *Mtb*-specific CD4⁺ and CD8⁺ T-cell PD-1 but not HLA-DR expression in LTBI-DM participants

Next, to characterise the *Mtb*-specific exhaustion and activation profiles of CD4⁺ and CD8⁺ T-cells, we determined the expression profiles of PD-1 and HLA-DR (Fig. 4A and E). For LTBI-DM participants, CD4⁺ and CD8⁺ T-cell PD-1 expression was significantly downregulated post-IPT [32.75 (11.80–42.80): 24.70 (9.95–38.43); $p = 0.042$] and [26.00 (16.23–40.38): 20.05 (12.48–35.18); $p = 0.031$], respectively (Fig. 4B and F). The HC participants exhibited significantly lower CD4⁺ PD-1 expression compared to LTBI-DM participants at baseline [16.70 (13.60–20.40); $p = 0.018$] (Fig. 4B), indicating a trend toward normalisation post-IPT in LTBI-DM participants for CD4⁺ T cells. Conversely, CD4⁺ and CD8⁺ T-cell HLA-DR expression did not differ before and post-IPT for LTBI-DM participants [0.91 (0.56–1.91): 0.83 (0.65–2.57); $p = 0.107$] and [0.95 (0.68–1.30): 1.11 (0.66–1.98); $p = 0.331$)], respectively (Fig. 4C and G). Notably, HC participants showed significantly upregulated HLA-DR expression compared to LTBI-DM at both M0 [CD4⁺: 2.53 (1.85–3.31), $p = 0.006$; CD8⁺: 1.84 (1.58–2.30), $p = 0.006$] and M6 [CD4⁺: $p = 0.013$] (Fig. 4C and G). Additionally, for LTBI-DM participants, CD8⁺ T-cell CD107a production was significantly increased post-IPT [1.59 (0.94–2.40): 2.16 (1.36–3.14); $p = 0.037$] (Fig. 4H), while CD4⁺ T-cell CD107a was non-significant post-IPT [0.57 (0.52–0.98): 0.78 (0.55–1.29); $p = 0.360$] (Fig. 4D).

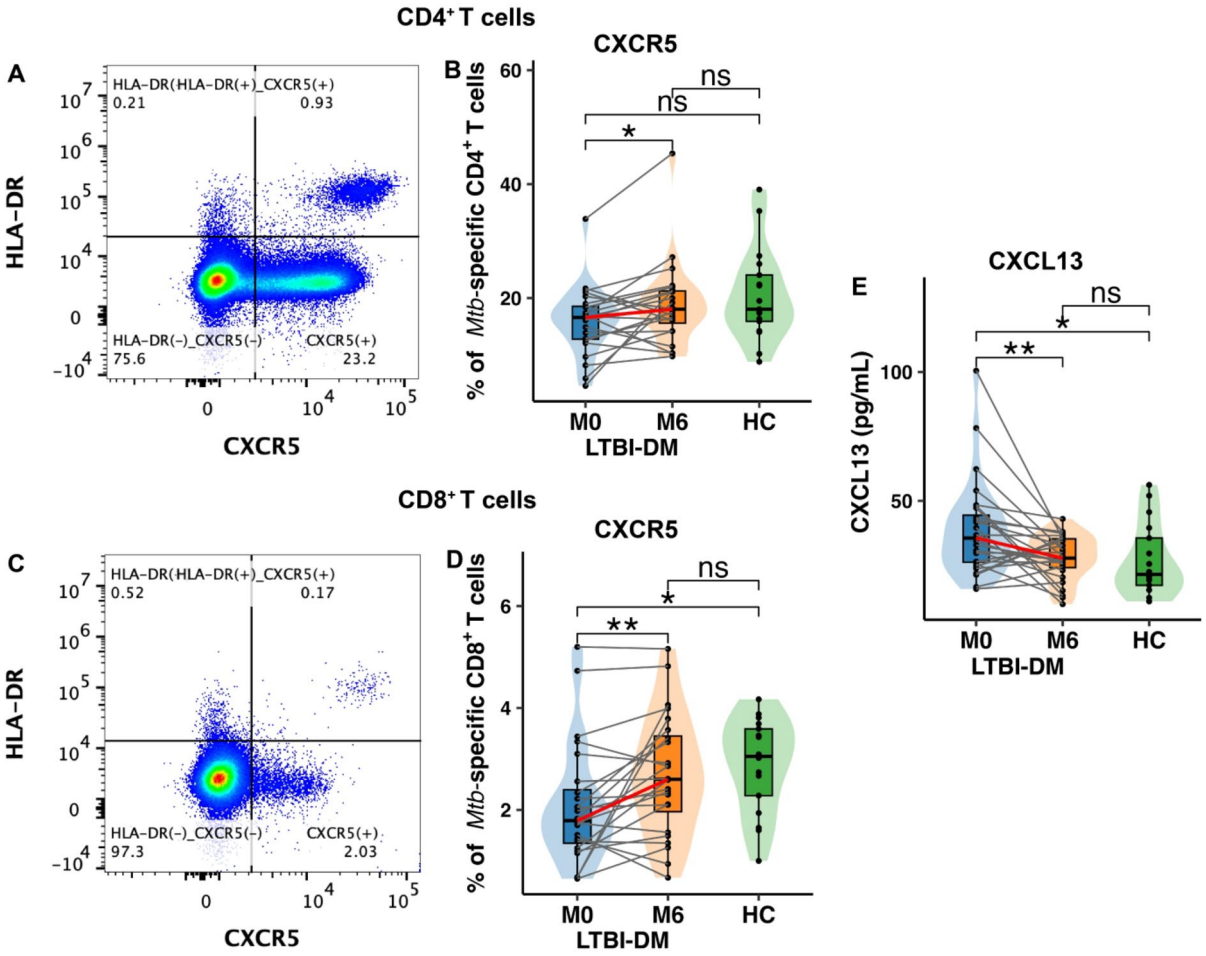

Fig. 3. *Mtb*-specific CD4⁺ and CD8⁺ T-cell CXCR5 and CXCL13 expression profiles before and after IPT for LTBI-DM; and HC participants.

The HC participants showed significantly upregulated CD4⁺ CD107a production [1.30 (0.82–2.20)] compared to LTBI-DM at M0 ($p = 0.003$) and M6 ($p = 0.024$) (Fig. 4D).

Representative flow cytometry plots are shown for (A and E) CD4⁺ and CD8⁺ PD-1, HLA-DR, and CD107a functional profiles. PBMCs were stimulated and cultured for 18 h with ESAT-6 and CFP-10 peptide pools plus brefeldin A and stained for surface markers. (B-D and F-H) Representative combined dot-violin-box plots that depict the percentage expression of PD-1, HLA-DR, and CD107a functional profiles in CD4⁺ and CD8⁺ T cells in LTBI-DM; and HC participants. The grey lines depict individual participant phenotype trajectories from M0 to M6, while the red line represents the aggregate median trend for LTBI-DM participants over the same period. Size of group: LTBI-DM ($n = 24$), HC ($n = 17$). Wilcoxon matched-pairs signed rank and Mann-Whitney U tests were performed to determine the statistical significance between M0 and M6 for LTBI-DM, as well as between HC and M0/M6, respectively. $p < 0.05$ (*), $p < 0.01$ (**). Non-significant (ns) p-values were not shown.

IPT upregulates *Mtb*-specific CD4⁺ T-cell IL-17 A and CD8⁺ T-cell IL-13 production but not IFN-γ in LTBI-DM participants

To further assess the quality of CD4⁺ and CD8⁺ T-cell responses, we determined the *Mtb*-specific production of cytokines (IFN-γ, IL-13 and IL-17 A) by the two subsets. Among LTBI-DM participants, CD4⁺ T-cell IL-17 A production was upregulated post-IPT [0.49 (0.20–0.69): 1.01 (0.63–1.31); $p = 0.004$] (Fig. 5C). This post-IPT IL-17 A production was comparable to the higher levels observed in HC participants [0.97 (0.71–1.47); $p = 0.001$] compared to LTBI-DM participants at baseline (Fig. 5C). Although CD4⁺ T-cell IFN-γ and IL-13 production in LTBI-DM participants was non-significant post-IPT [0.57 (0.24–0.85): 0.53 (0.32–0.90)] and [0.33 (0.14–0.61): 0.50 (0.27–0.86)], respectively, IFN-γ production in HC participants was significantly lower than in LTBI-DM participants at M6 [0.27 (0.17–0.43); $p = 0.040$] (Fig. 5A and B). For LTBI-DM participants, CD8⁺ T-cell IL-13 production was significantly upregulated post-IPT [0.45 (0.23–0.79): 0.80 (0.52–1.20); $p = 0.033$] (Fig. 5E). In addition, CD8⁺ T-cell production IFN-γ and IL-17 A production was not upregulated post-IPT (Fig. 5D and F). Conversely, CD8⁺ T-cell IFN-γ [0.52 (0.28–1.29)] production at baseline in LTBI-DM participants was significantly higher compared to HC participants [1.27 (0.75–2.05); $p = 0.040$], with no changes post-IPT (Fig. 5D).

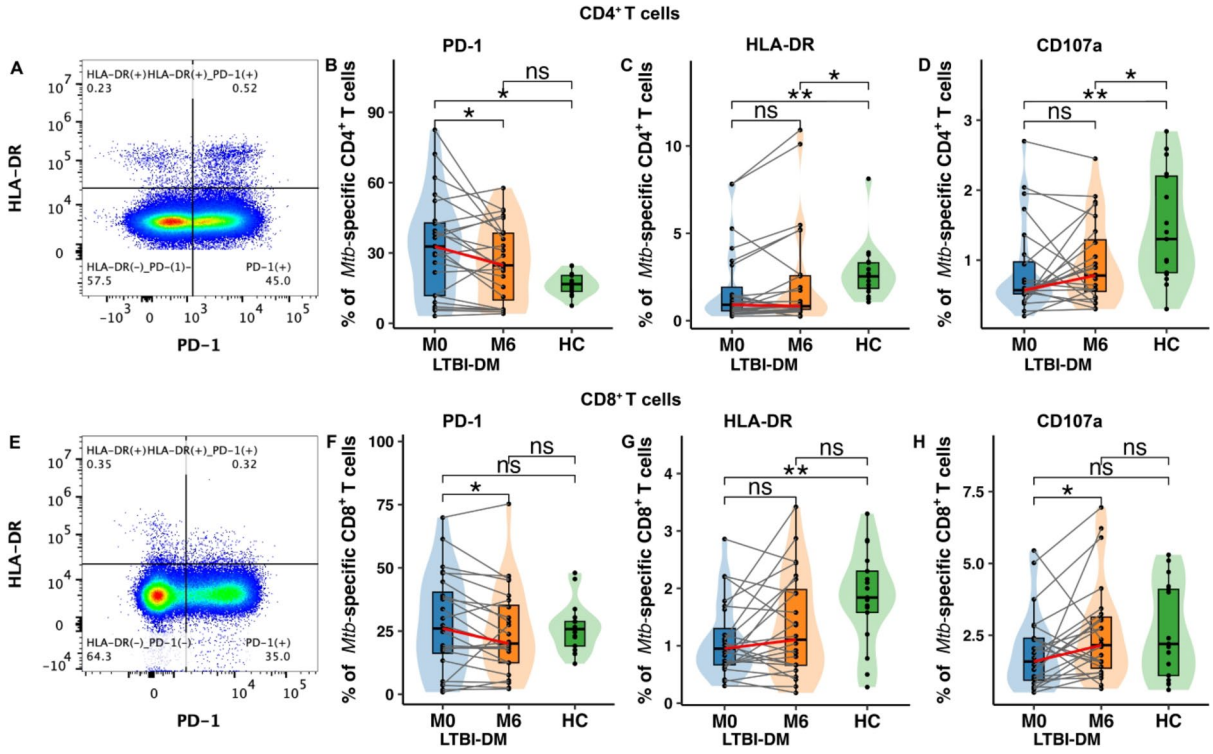

Fig. 4. *Mtb*-specific CD4⁺ and CD8⁺ T-cell PD-1, HLA-DR, and CD107a before and after IPT for LTBI-DM; and HC participants.

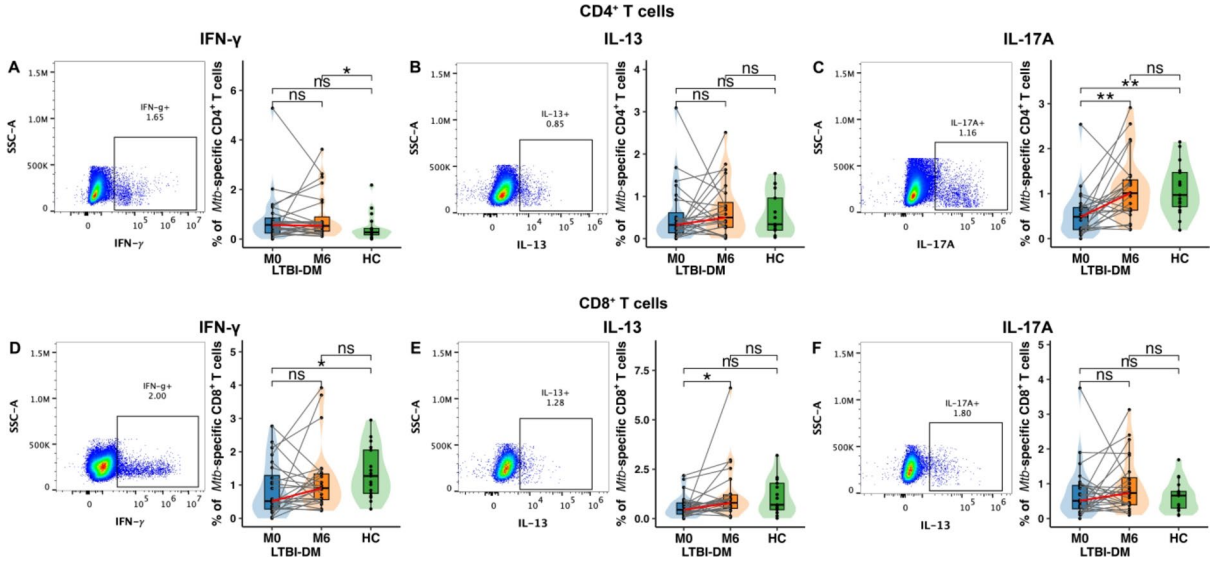

Fig. 5. *Mtb*-specific CD4⁺ and CD8⁺ T-cell cytokine profiles before and after IPT for LTBI-DM; and HC participants.

Representative flow cytometry plots are shown for (A and D) CD4⁺ and CD8⁺ T-cell IL-17 A and IL-13 cytokine profiles, respectively. PBMCs were stimulated and cultured for 18 h with ESAT-6 and CFP-10 peptide pools plus brefeldin A and stained for intracellular markers. (B-C and E-F) Representative combined dot-violin-box plots depicting the percentage expression of cytokine profiles in CD4⁺ and CD8⁺ T-cell IFN-γ, IL-13 and IL-17 A cytokine profiles in LTBI-DM; and HC participants. The grey lines depict individual participant phenotype trajectories from M0 to M6, while the red line represents the aggregate median trend for LTBI-DM participants over the same period. Size of group: LTBI-DM ($n = 24$), HC ($n = 17$). Wilcoxon matched-pairs signed rank and

Mann-Whitney U tests were performed to determine the statistical significance between M0 and M6 for LTBI-DM, as well as between HC and M0/M6, respectively. $p < 0.05$ (*), $p < 0.01$ (**).

Discussion

We analysed the memory phenotypes and functional characteristics of *Mtb*-specific CD4$^+$ and CD8$^+$ T cells of LTBI-DM participants before and after IPT, with additional comparisons to HC participants to evaluate whether IPT could restore T-cell responses towards a healthy baseline. Our data show that IPT decreases *Mtb*-specific CD4$^+$ and CD8$^+$ T-cell effector memory phenotypes, increases *Mtb*-specific CD4$^+$ and CD8$^+$ T-cell CXCR5 expression, decreases CXCL13 protein expression levels and *Mtb*-specific CD4$^+$ and CD8$^+$ T-cell PD-1 expression. These data supplement our current knowledge of *Mtb*-specific immune responses post-IPT in LTBI-DM participants otherwise studied in active TB and DM participants[17].

The phenotypic and functional heterogeneity of CD4$^+$ and CD8$^+$ T cells is essential in determining whether these cells are protective[19]. CD4$^+$ and CD8$^+$ memory T cells play critical roles in protective immunity against TB[20–22]. Moreover, latent TB infection is associated with the expansion of effector and central memory T cells[23]. Our study reports that effector memory T cells, crucial for immediate and rapid *Mtb*-specific immune responses[24], significantly decreased in CD4$^+$ and CD8$^+$ subsets post-IPT in LTBI-DM participants. Importantly, these effector memory T-cell post-IPT reductions were comparable to those observed in HC participants, suggesting a potential for their rebalancing upon IPT completion in LTBI-DM participants. These results are consistent with studies of active TB that reported decreased frequencies of effector memory CD4$^+$ T cells and increased frequencies of central memory CD4$^+$ T cells after TB treatment[16,25]. The reduction of effector memory T cells may indicate a shift in the immune landscape, potentially reflecting a decreased immediate need for such rapid responses due to the lowered risk of active TB following IPT. The decreased effector memory T-cell frequencies could also indicate increased differentiation of T-cell memory phenotypes into other T-cell phenotypes post-IPT[24]. This warrants further studies to determine the fate of the differentiated phenotypes post-IPT. It could also reflect the migration patterns of these memory subsets, for which an influx of effector memory T cells into the lung would increase the peripheral distribution of the central memory T cells. The effector memory T-cell decline could influence the overall effectiveness of the immune defence against latent tuberculosis reactivation[25].

Next, we assessed the lung homing and exhaustion capacities of CD4$^+$ and CD8$^+$ T cells in LTBI-DM participants. During TB infection within the mouse and human lungs, CXCL13 induction and its interaction with CXCR5 contributes to the recruitment and organisation of lymphocytes within the inducible Bronchus-associated lymphoid structures (iBALT) of the granuloma[26,27]. Consistent with this, both CD4$^+$ and CD8$^+$ T-cell CXCR5 expression levels were significantly upregulated post-IPT for LTBI-DM participants, reaching levels comparable to those of HC participants, who showed markedly enhanced CD8$^+$ T-cell CXCR5 expression. Conversely, the high CXCL13 protein levels in LTBI-DM participants significantly decreased post-IPT, comparable to those in HC participants. This is consistent with results that showed decreased CXCL13 expression levels after TB treatment[28]. The upregulation of the T-cell CXCR5 expression suggests an enhanced ability for these cells to migrate to lymphoid follicles, where immune responses against *Mtb* may be initiated and regulated[26,27]. Conversely, the reduction in plasma systemic CXCL13 levels post-IPT indicates a potential modulation of granuloma formation and organisation within lymphoid tissues, which could impact the overall immune milieu and subsequent immune responses against *Mtb*[26,29]. During TB infection, PD-1 expression on *Mtb*-specific T cells is associated with bacterial load[30]. Surprisingly, our study shows that LTBI-DM participants had a reversal of T-cell exhaustion post-IPT. Interestingly, the post-IPT PD-1 expression approached normal levels seen in HC participants. Exhausted T cells are characterised by impaired cell function and proliferation[31,32]. Isoniazid preventive therapy could have lowered the bacterial burden, which resulted in a low expression of PD-1 on *Mtb*-specific CD4$^+$ and CD8$^+$ T cells, as seen in HC participants. This could have reversed T-cell dysfunction, upregulating the expression of CXCR5, IL-17 A and IL-13 production by *Mtb*-specific T cells. Our results for the reversal of T-cell exhaustion are similar to those reported in other studies for TB treatment and anti-PD-1 immunotherapy[16,33].

Moreover, our investigation into cytokine production by the *Mtb*-specific CD4$^+$ and CD8$^+$ T cells yielded intriguing findings regarding the effects of IPT on the quality of T-cell responses. IL-17-specific CD4$^+$ T cells have been reported to contribute to human anti-mycobacterial immune responses[34]. Interestingly, CD4$^+$ T cells expressing IL-17 A have recently been shown to correlate with reduced *Mtb* lung burden[35]. The upregulation of IL-17 A production by *Mtb*-specific CD4$^+$ T cells post-IPT in LTBI-DM participants (similar to HC) suggests a potential shift towards a Th17-mediated immune response, which has been implicated in the protection against *Mtb*[34,35]. Similarly, the significant increase in IL-13 production by *Mtb*-specific CD8$^+$ T cells post-IPT in LTBI-DM participants (similar to HC) highlights the complexity of the immune response to *Mtb* antigens[36].

However, it is important to interpret these findings within the context of the limitations of our study. This preliminary work brings to light some of the initial evidence of immune responses associated with IPT among the DM population. However, bigger studies with longer follow-up time will provide more substantive evidence on the effects of TPT in DM and the durability of such effects. Also, the immunomodulatory effects of diabetes and metformin on tuberculosis immunity[37], coupled with the potential interactions between anti-diabetic medications and IPT, suggest the need for comprehensive phenotypic and functional analyses to elucidate the underlying mechanisms driving the observed changes in the *Mtb*-specific T-cell responses. This study did not comprehensively assess for T-cell exhaustion (e.g., LAG-3, TIM-3, CTLA-4) and polyfunctionality (e.g., TNF, IL-2) markers. Finally, our study did not have an LTBI-only group that received IPT because, at its conception, LTBI-only participants without a clinically indicated risk (for example, children under 5 years and those living with HIV) do not receive IPT unless for clinical trials. This hindered the study's ability to determine the effects of IPT regardless of DM status.

In conclusion, our study provides valuable insights into the impact of IPT on *Mtb*-specific T-cell responses in individuals with comorbid latent TB infection and type 2 diabetes mellitus. The observed alterations in T-cell memory phenotype, homing capabilities, exhaustion, and cytokine production highlight the complex immunological dynamics underlying tuberculosis immunity and the potential of IPT as a modulator of T-cell-mediated immune responses towards normal levels. Further studies are warranted to validate these findings and elucidate the underlying mechanisms driving these immunological changes, aiming to optimise therapeutic strategies for tuberculosis prevention and control in high-burden settings.

Data availability

The datasets supporting the conclusions of this article are available from the corresponding author upon reasonable request.

Received: 21 December 2024; Accepted: 20 March 2025
Published online: 26 March 2025

References

1. Jeon, C. Y. & Murray, M. B. Diabetes mellitus increases the risk of active tuberculosis: a systematic review of 13 observational studies. *PLoS Med.* **5**(7), e152 (2008).
2. World Health Organisation. *Global Tuberculosis Report 2024* (WHO, 2024).
3. Ssekamatte, P. et al. Type 2 diabetes mellitus and latent tuberculosis infection moderately influence innate lymphoid cell immune responses in Uganda. *Front. Immunol.* ;**12**(3551), 716819 (2021).
4. Ssekamatte, P., Sande, O. J., van Crevel, R. & Biraro, I. A. Immunologic, metabolic and genetic impact of diabetes on tuberculosis susceptibility. *Front. Immunol.* ;**14**, 1122255 (2023).
5. Kumar, N. P. et al. Diminished systemic and antigen-specific type 1, type 17, and other Proinflammatory cytokines in diabetic and prediabetic individuals with latent Mycobacterium tuberculosis infection. *J. Infect. Dis.* **210**(10), 1670–1678 (2014).
6. Kumar, N. P. et al. Profiling leucocyte subsets in tuberculosis-diabetes co-morbidity. *Immunology* **146**(2), 243–250 (2015).
7. Mogues, T., Goodrich, M. E., Ryan, L., LaCourse, R. & North, R. J. The relative importance of T cell subsets in immunity and immunopathology of airborne Mycobacterium tuberculosis infection in mice. *J. Exp. Med.* **193**(3), 271–280 (2001).
8. Flynn, J. L. et al. An essential role for interferon gamma in resistance to Mycobacterium tuberculosis infection. *J. Exp. Med.* **178**(6), 2249–2254 (1993).
9. Crevel Rv, Ottenhoff, T. H. M., Meer & JWMvd Innate immunity to Mycobacterium tuberculosis. *Clin. Microbiol. Rev.* **15**(2), 294–309 (2002).
10. Cooper, A. M. Cell-mediated immune responses in tuberculosis. *Annu. Rev. Immunol.* **27**, 393–422 (2009).
11. Giese, I-M. et al. Chronic hyperglycemia drives functional impairment of lymphocytes in diabetic INSC94Y Transgenic pigs. *Front. Immunol.* **11**, 607473 (2021).
12. Nojima, I. et al. Dysfunction of CD8 + PD-1 + T cells in type 2 diabetes caused by the impairment of metabolism-immune axis. *Sci. Rep.* **10**(1), 14928 (2020).
13. Ssekamatte, P. et al. Impaired Mycobacterium tuberculosis-specific T-cell memory phenotypes and functional profiles among adults with type 2 diabetes mellitus in Uganda. *Front. Immunol.* **15**, 1480739 (2024).
14. Kumar, N. P. et al. Impaired cytokine but enhanced cytotoxic marker expression in Mycobacterium tuberculosis–Induced CD8 + T cells in individuals with type 2 diabetes and latent Mycobacterium tuberculosis infection. *J. Infect. Dis.* **213**(5), 866–870 (2016).
15. Teixeira, L. A. A. et al. Long-Term protective effect of tuberculosis preventive therapy in a medium/high tuberculosis incidence setting. *Clin. Infect. Dis.* **78**(5), 1321–1327 (2024).
16. Saharia, K. K. et al. Tuberculosis therapy modifies the cytokine profile, maturation State, and expression of inhibitory molecules on Mycobacterium tuberculosis-Specific CD4 + T-Cells. *PLOS ONE.* **11**(7), e0158262 (2016).
17. Kumar, N. P., Moideen, K., Viswanathan, V., Kornfeld, H. & Babu, S. Effect of standard tuberculosis treatment on Naive, memory and regulatory T-cell homeostasis in tuberculosis–diabetes co-morbidity. *Immunology* **149**(1), 87–97 (2016).
18. Biraro, I. A. et al. Impact of Co-Infections and BCG immunisation on immune responses among household contacts of tuberculosis patients in a Ugandan cohort. *PLOS ONE.* **9**(11), e111517 (2014).
19. Seder, R. A., Darrah, P. A. & Roederer, M. T-cell quality in memory and protection: implications for vaccine design. *Nat. Rev. Immunol.* **8**(4), 247–258 (2008).
20. Wang, J., Santosuosso, M., Ngai, P., Zganiacz, A. & Xing, Z. Activation of CD8 T cells by mycobacterial vaccination protects against pulmonary tuberculosis in the absence of CD4 T cells1. *J. Immunol.* **173**(7), 4590–4597 (2004).
21. Silva, B. & Lima, Faccioli, L. Characterization of the memory/activated t cells that mediate the long-lived host response against tuberculosis after Bacillus Calmette–Guérin or DNA vaccination. *Immunology* **97**(4), 573–581 (1999).
22. Lindestam Arlehamn, C. S. et al. Memory T cells in latent Mycobacterium tuberculosis infection are directed against three antigenic Islands and largely contained in a CXCR3 + CCR6 + Th1 subset. *PLoS Pathog.* **9**(1), e1003130 (2013).
23. Pollock, K. M. et al. T-Cell immunophenotyping distinguishes active from latent tuberculosis. *J. Infect. Dis.* **208**(6), 952–968 (2013).
24. Arrigucci, R. et al. Active tuberculosis is characterized by highly differentiated effector memory Th1 cells. *Front. Immunol.* **9**, 02127 (2018).
25. Chiacchio, T. et al. Impact of antiretroviral and tuberculosis therapies on CD4 + and CD8 + HIV/M. tuberculosis-specific T-cell in co-infected subjects. *Immunol. Lett.* **198**, 33–43 (2018).
26. Slight, S. R. et al. CXCR5 + T helper cells mediate protective immunity against tuberculosis. *J. Clin. Investig.* **123**(2), 712–726 (2013).
27. Hoft, S. G. et al. The rate of CD4 T cell entry into the lungs during Mycobacterium tuberculosis infection is determined by partial and opposing effects of multiple chemokine receptors. *Infect. Immun.* **87**(6). https://doi.org/10.1128/iai.00841 (2019).
28. Ardain, A. et al. Group 3 innate lymphoid cells mediate early protective immunity against tuberculosis. *Nature* **570**(7762), 528–532 (2019).
29. Ulrichs, T. et al. Human tuberculous granulomas induce peripheral lymphoid follicle-like structures to orchestrate local host defence in the lung. *J. Pathol.* **204**(2), 217–228 (2004).
30. Day, C. L. et al. PD-1 expression on Mycobacterium tuberculosis-Specific CD4 T cells is associated with bacterial load in human tuberculosis. *Front. Immunol.* **9**, 01995 (2018).
31. Wherry, E. J. T cell exhaustion. *Nat. Immunol.* **12**(6), 492–499 (2011).
32. Shen, L. et al. PD-1/PD-L pathway inhibits M.tb-specific CD4 + T-cell functions and phagocytosis of macrophages in active tuberculosis. *Sci. Rep.* **6**(1), 38362 (2016).
33. Tezera, L. B. et al. Anti-PD-1 immunotherapy leads to tuberculosis reactivation via dysregulation of TNF-α. *eLife* **9**, e52668 (2020).

34. Scriba, T. J. et al. Distinct, specific IL-17- and IL-22-Producing CD4 + T cell subsets contribute to the human Anti-Mycobacterial immune Response1. *J. Immunol.* **180**(3), 1962–1970 (2008).
35. Stewart, E. L. et al. Lung IL-17A-Producing CD4 + T cells correlate with protection after intrapulmonary vaccination with differentially adjuvanted tuberculosis vaccines. *Vaccines* **12**(2), 128 (2024).
36. Amelio, P. et al. Mixed Th1 and Th2 Mycobacterium tuberculosis-specific CD4 T cell responses in patients with active pulmonary tuberculosis from Tanzania. *PLoS Negl. Trop. Dis.* **11**(7), e0005817 (2017).
37. Van Crevel, R., Koesoemadinata, R., Hill, P. & Harries, A. Clinical management of combined tuberculosis and diabetes. *Int. J. Tuberc. Lung Dis.* **22**(12), 1404–1410 (2018).

Acknowledgements

We are grateful to the study participants under Kiruddu National Referral Hospital, and Kisenyi and Kitebi Health Center IVs. We are grateful to BEI resources, NIAID, NIH for supplying us with the Peptide Array, Mycobacterium tuberculosis ESAT-6 Protein, NR-50711, and CFP-10 Protein, NR-50712. We also thank the Makerere University Walter Reed Project (MUWRP) flow cytometry laboratory team for providing laboratory space to perform all flow cytometry incubations. Lastly, we thank PROTID clinical trial (grant number: RIA-2018CO-2514), an EDCTP2 programme supported by the European Union and the Government of Uganda through the Uganda Independence Scholarship Trust Fund (UISTF) for the support.

Author contributions

PS, OJS, RvC SC, and IAB conceptualised the study. PS, DS and RN conducted the experiments. PS analysed data. DS, RN, MN, BSB, DK, APK, DPK, OJS, RvC, SC, and IAB thoroughly reviewed the results. The first draft of the manuscript was written by PS, which was later reviewed for intellectual content input by DS, RN, MN, BSB, DK, APK, DPK, OJS, RvC, SC, and IAB. All authors approved the final version of the manuscript for publication.

Funding

This project was mainly supported by postdoctoral fellowships from Makerere University/UVRI Centre of Excellence in Infection and Immunity Research and Training (MUII Plus; grant number 084344) and the MRC/UVRI and LSHTM Uganda Research Unit training grant, both held by Prof. Irene Andia Biraro. Further funding and support was through the MRC/UVRI and LSHTM Uganda Research Unit, which is jointly funded by the UK Medical Research Council (MRC) part of UK Research and Innovation (UKRI) and the UK Foreign, Commonwealth and Development Office (FCDO) under the MRC/FCDO Concordat agreement and also part of the EDCTP2 programme supported by the European Union.

Declarations

Competing interests

The authors declare no competing interests.

Additional information

Correspondence and requests for materials should be addressed to P.S.

Reprints and permissions information is available at www.nature.com/reprints.

Publisher's note Springer Nature remains neutral with regard to jurisdictional claims in published maps and institutional affiliations.